Original Scientific article
http://dx.doi.org/10.59456/afts.2023.1529.023C

TIME DEPENDENT DEFORMATIONS OF A COUPLED BRIDGE: A CASE STUDY

Cumbo Anđelko[1], Folić Radomir[2]

[1]*Faculty of Architecture, Civil Engineering and Geodesy, University of Banjaluka, Republic of Srpska, Bosnia and Herzegovina, e-mail: andjelko.cumbo@aggf.unibl.org*
[2]*Department of Civil Engineering and Geodesy, Faculty of Technical Sciences, University of Novi Sad, Serbia*

ABSTRACT

The bridge's span structure comprises a connected beam designed to support a concrete slab poured over parallel steel supports. Simultaneously, segmental construction, shrinkage, and the flow of concrete play a significant role in stress redistribution over time. The span construction is statically indeterminate due to its connections with the abutments, and temporal deformations occur under additional complex conditions. In this analysis, we employed a calculation model based on the layered finite elements method developed by the authors. This model can be utilized to analyse both statically indeterminate supports and the predicted phased construction method. It accounts for changes in the static system and loading, as well as variations in the layers within the coupled section and the viscous properties of the concrete over time. The calculation analysis results reveal that viscous concrete deformations, combined with different moments of activation of individual segments, have a significant impact on stress redistribution over time. Such intricate analyses are indispensable for ensuring the required safety and cost-effectiveness of the bridge span construction.

Key words: *composite bridges, creep and shrinkage of concrete, phased construction, effective width, finite element method.*

INTRODUCTION AND SUMMARY OF LITERATURE

Coupled steel-concrete (CS-C) structures are commonly employed in both buildings and bridges. In bridges, it is typical to utilize span-jointed beams, which are created by pouring a concrete slab over parallel steel girders. Simultaneously, the connection between the steel supports and the concrete slab is established using tie rods. This approach results in the formation of a rational and cost-effective configuration for the span beam, leveraging the advantages of the high tensile load capacity of the steel support and the high compressive strength of the concrete [1]. This construction method yields beams characterized by significant load-bearing capacity and substantial rigidity [2]. The benefits of employing such structures manifest in terms of cost-effectiveness, construction speed, and safety. The composite cross-section consists of two distinct materials: steel, exhibiting elastic behaviour, and concrete, which displays viscous properties due to shrinkage and flow. These rheological phenomena in concrete induce alterations in internal forces, deflections, and their redistribution under the working loads applied to the coupled beam. This holds true for both statically determinate and statically indeterminate systems.

The international code provisions are used for the designing of composite bridges. In the USA it is [3], and in Europe those are, primarily, Eurocode [4] and [5], and in New Zealand, the reference [6] is used. Prediction and inclusion of the shrinkage and creep of concrete uses the provisions of [4] documents [7]

and [8], and in the USA [9], as well as the reference [10]. The comparative analysis of European and US codes is the subject matter of [10], for the creep function is suggested by the ACI [9]. Particularly important are the guidelines for the application of Eurocodes provided in [12] and [13]. A status review related to the conceptual designing of composite bridges (CB) is discussed in [14], and designing and analysis in [15].

The subject matter of the paper [1] is the review of the time-dependent behaviour of CS-C bridges, and the general design approach, along with the analysis of the construction phases were described in [16]. Effects of time-dependent behaviour of concrete based on the coupling of the FEM with a numerical solution of the hereditary Volterra integral equations were discussed. A similar paper is also [17] in which the effects temperature changing and concrete creep CS-C bridges and behaviour during construction and operation periods were discussed. The master theses [18] are also worth mentioning, as they provide general consideration on the designing of CS-C bridges, and in [19] are present the analysis of the effects of shrinkage and creep of concrete in S-C composite beams, mainly based on the use of Eurocodes. In the paper [20] are considered the effects of redistribution in the linear elastic analysis of a continuous composite beam according to Eurocode 4, and in the paper [21] there is a non-linear analysis of the time-dependent behaviour of a composite beam. A mixed FE model for nonlinear analysis with partial shear connection was used and it was shown that the interaction between cracking and time effects significantly increases the deformation. The factors affecting the shrinkage and creep of concrete and the guidelines for their modelling were described in [22], and there are also useful data in the Proceedings of the workshop [23].

In the analysis of the composite steel-concrete bridges is used the effective width of the slab in order to employ the linear elements in the bridge analysis. It was stipulated in the provisions of Eurocode 4, and a more accurate analysis was presented in the papers [24,25,26]. In [25] it was indicated that the results calculated according to EN 1994 are not always sufficiently conservative, so significant structures require an in-detail analysis, most often created using the Finite Element Method. A comparative analysis of the expressions for determining the effective width recommended in the AASHTO, EC54, and norms of Brazil and China is presented in [30]. Also, it is recommended to use the reference [8] for the assessment of creep and shrinkage rate, and the use of the ACI model predicted the highest concrete shrinkage.

The results of the extensive research from Australia, about the time-dependent behaviour of a composite simple beam were described in the Report [27]. Similar results were presented in the paper [28]. The effects of time-dependent deformations for the perfect connection of the steel beam and the concrete slab were described in [29]. Results of the finite element method analysis for the ultimate limit state, and time-dependent behaviour were presented in [30]. The results of the analysis of simulation methods using the finite element method are the subject of the paper [31]. In the paper [32] the simplified analysis methodology was described, and the accuracy aspect of the results was discussed. In the paper [33] a simplified algorithm for the simple composite beam was developed, and in the paper [34] the experimental results for the negative zone of bending moments of the specially reinforced road deck were described. The subject of the paper [35] is studying the impact of the shear creep for the analysis of long-term deformations of a long span concrete beam. A special case of formation of composite beams, Preflex and Flexstress beams, with different phases of formation of composite beams and their analysis were provided in the paper [36]. Steel I beams, in addition to the top reinforced concrete slab also have a bottom slab, i.e., concreted bottom flange.

One of the composite bridges is the subject of this paper, and it is the new road bridge across the Vrbas river on the approach to the city of Banjaluka (B and H) which was in accordance with the local prescribed requirements, technical norms and professional rules (Figure 1). The bridge is located perpendicular to the river, having a static span of 6.0+50.0+6.0 m, with a two-way traffic, and the total width of 11.0 m. The shallow foundations of caisson abutments lie on the soil having sound engineering and geological properties. The spanning structure is a continuous steel-concrete composite beam (two steel I beams of variable height 160-250 cm, with transverse beams and stiffeners; the 25-35 cm thick reinforced concrete (RC) road deck was concreted on top of this structure. The spanning structure is in fact an elastically restrained beam. The length of the medium span is considerably higher than the end spans, which forms a couple reactions in the abutments. These reactions are absorbed by the massive

caisson abutments which act as counterweights during the console construction of the bridge, but also in operation. The position, symmetrical proportions and appearance of the bridge make it fit well into the natural environment of the location.

Figure 1. Road bridge over the Vrbas river, Banjaluka

During the development of the project, the authors performed a control calculation analysis of the stress-deformation state of the coupled span structure of the bridge. All relevant phases which included the segmental procedure of construction with a special emphasis on shrinkage and creep of concrete were analysed.

In this paper, in addition to a brief review of the literature, the theoretical bases for the analysis, which were previously developed by the author, are briefly presented [37,38]. The necessary input data for the analysis were listed, as well as the results of calculation for the composite spanning structure – beam. The results for all the phases of analysis were discussed, and based on them the appropriate conclusions were drawn.

ANALYSIS METHODOLOGY

Theoretical Basis for Calculating the Effects of Shrinkage and Flow of Concrete

Bridges are often constructed in phases using coupled steel-concrete span structures. These phases involve changes in the geometry of the elements, the static system, and the loads at various time intervals, resulting in alterations in the state of stress and deformation within the elements. The shrinkage and flow of concrete, along with the emergence of cracks in the tensioned zone, lead to a redistribution of stresses and deformations in the coupled structure. This necessitates the introduction of varying time intervals for the inclusion or exclusion of individual elements or their layers in tension activities, taking into account all their viscoelastic material properties. This is crucial due to the phased construction process and, additionally, the static indeterminacy of the structure, which can lead to changes in forces within the structure without altering the external load.

To address these challenges, the authors developed a computational algorithm utilizing layered finite elements (FE) [37] and [38]. Through appropriately defined layers, the rheological properties of concrete are incorporated in the form of a fictitious load, enabling the analysis of statically indeterminate coupled structures. Incremental forms of the stress-strain relationship were applied to all different materials. The computational algorithm accommodates both discontinuous and continuous changes (in the static system, geometry, load, and rheology) across fictitious ($\Delta t_k = 0$) and finite ($\Delta t_k \neq 0$) time intervals. The solution is obtained by solving a system of algebraic equations in matrix form using the finite element method (FEM). This computational algorithm has been validated against a substantial number of examples from the literature, confirming a very good agreement of the results.

In general, the calculation model comprises rigidly coupled layered elements and assumes a linear stress-strain relationship for concrete ($\sigma_c \leq 0.4 f_{ck}$), adhering to the hypothesis of flat sections and the linear theory of concrete flow.

In the expressions presented here, symbols are introduced for common materials constituting the coupled elements (a-structural steel, c-concrete, s-reinforcement), Therefore, the deformation of the observed fiber within the coupled cross-section during the current time interval (Δt_k) is valid for the incremental equation (in matrix form):

$$\Delta\varepsilon_k = [\Delta\varepsilon_r \quad \Delta\kappa]_k \cdot \begin{vmatrix} 1 \\ y \end{vmatrix}_k \tag{1}$$

Here:

$\Delta\varepsilon_k$ – Deformation of the observed fiber cross-section,
$\Delta\varepsilon_{r,k}$ – Expansion of the fiber at the level of the reference axis of the cross-section ($y = 0$),
$\Delta\kappa_k$ – Curvature of the cross-section,
y – Distance of the observed fiber from the reference axis r.

For the adopted linear relationship between stress parameters ($\Delta\alpha_{r,k}$ and $\Delta\beta_k$) and deformation ($\Delta\varepsilon_{r,k}$ and $\Delta\kappa_k$), the constitutive relationship for structural steel and reinforcement (both elastic materials) is as follows:

$$\begin{vmatrix} \Delta\alpha_r \\ \Delta\beta \end{vmatrix}_{a,k} = E_a \cdot \begin{vmatrix} \Delta\varepsilon_r \\ \Delta\kappa \end{vmatrix}_{a,k} \quad ; \quad \begin{vmatrix} \Delta\alpha_r \\ \Delta\beta \end{vmatrix}_{s,k} = E_s \cdot \begin{vmatrix} \Delta\varepsilon_r \\ \Delta\kappa \end{vmatrix}_{s,k} \tag{2}$$

The constitutive relationship for concrete (a viscous material) takes the following form:

$$\begin{vmatrix} \Delta\alpha_r \\ \Delta\beta \end{vmatrix}_{c,k} = E_{c(k,k-1)} \cdot \left(\begin{vmatrix} \Delta\varepsilon_r \\ \Delta\kappa \end{vmatrix} - \begin{vmatrix} \Delta\varepsilon_r^* \\ \Delta\kappa^* \end{vmatrix} \right)_{c,k} \tag{3}$$

In contrast to structural and reinforcing steel, which are assumed to exhibit elastic stress-strain relationships, concrete, as a viscous material, introduces an additional deformation known as "free deformation." This accounts for viscous time-dependent deformations as follows:

$$\begin{vmatrix} \Delta\varepsilon_r^* \\ \Delta\kappa^* \end{vmatrix}_{c,k} = \sum_{i=1}^{k-1} \frac{1}{E^*_{c(k,i-1)}} \cdot \begin{vmatrix} \Delta\alpha_r \\ \Delta\beta \end{vmatrix}_{c,i} + \begin{vmatrix} \Delta\varepsilon_{cs} \\ 0 \end{vmatrix}_k \tag{4}$$

Here:

$E_{c(k,k-1)}$ – Effective generalized concrete deformation modulus.,
$E^*_{c(k,i-1)}$ – Effective derived concrete deformation modulus,
$\Delta\varepsilon_{cs,k}$ – Deformation due to shrinkage of concrete (constant for the height of the cross-section).

The deformation moduli depend on the concrete yield function applied and the type of numerical integration, following the relationship:

$$\frac{1}{E^*_{c(k,i-1)}} = \frac{1}{E_{c(k,i-1)}} - \frac{1}{E_{c(k-1,i-1)}} \quad ; \quad i = 1,2,\dots,k-1 \tag{5}$$

The generalized form of the constitutive stress-strain relation (3) allows for the application of various concrete flow function forms. The AAEM method [10] is implemented as follows:

$$\frac{1}{E_{c(k,i-1)}} = 1 + \chi_{(k,i-1)} \cdot \varphi_{(k,i-1)} \quad ; \quad i = 1,2,\dots,k \tag{6}$$

Here:

$\chi_{(k,i-1)}$ – Correction coefficient of concrete flow (aging coefficient),
$\varphi_{(k,i-1)}$ – Flow coefficient of concrete, $(i = 1,2,\dots,k)$.

Expression (4) calculates the "free deformations" of the concrete within the k-th interval, considering stress from all previous intervals Δt_i, $(i = 1,2,\dots,k-1)$, and the deformations from the shrinkage of

concrete that takes place in the current interval (Δt_k). This approach unifies calculations across all fictitious and finite time intervals, accounting for varying geometric and material properties and external influences.

The incremental relationship between deformation and forces in the cross-section can be expressed as follows:

$$\mathbf{K}_k \cdot \left|\begin{matrix}\Delta\varepsilon_r \\ \Delta\kappa\end{matrix}\right|_k = \left|\begin{matrix}\Delta N \\ \Delta M\end{matrix}\right|_k - \left|\begin{matrix}\Delta N^* \\ \Delta M^*\end{matrix}\right|_{c,k} \tag{7}$$

Here:

K_k – Matrix of stiffness for the coupled cross-section (the sum of contributions from steel, reinforcement, and concrete),

ΔN_k , ΔM_k – Normal force and bending moment in the cross-section due to external loads,

$\Delta N^*_{c,k}$, $\Delta M^*_{c,k}$ – Fictitious normal force and fictitious bending moment in the cross-section resulting from shrinkage and flow of concrete.

For statically determined supports, it would be sufficient to use expression (7) because it allows for the determination of deformations and normal stresses in the cross-section. However, in the case of statically undetermined constructions, forces within the cross-sections change due to the rheological properties of the concrete, even when there is no change in the external load. In such cases, calculations of the state within the cross-section may not yield authoritative results. Therefore, there is a need to develop a complete construction algorithm, and for this purpose, the finite element method (FEM) is highly suitable.

In accordance with FEM principles, all parameters are associated with nodal points (e.g., displacements: $\Delta u, \Delta v, \Delta\varphi$, forces: $\Delta N, \Delta T, \Delta M$). For a single finite element (FE), the incremental relationship between the deformation magnitudes at the field points of the element ($\Delta\varepsilon_r$ and $\Delta\kappa$) and the displacement vector of its nodes ($\mathbf{\Delta q}_r$) is expressed as follows:

$$\left|\begin{matrix}\Delta\varepsilon_r \\ \Delta\kappa\end{matrix}\right|_k = \mathbf{B}_{r,k} \cdot \mathbf{\Delta q}_{r,k} \tag{8}$$

Here, $B_{r,k}$ represents the shape function, which is the element field matrix for the reference axis r.

By applying the established theoretical principles upon which the FEM is founded, we derive the fundamental equation for the coupled viscous FE in the following form:

$$\mathbf{K}_k \cdot \mathbf{\Delta q}_{r,k} = \mathbf{\Delta Q}_k - \mathbf{\Delta Q}^*_{\mathbf{c,k}} \tag{9}$$

Where:

K_k – Stiffness matrix of the coupled finite element (sum of contributions from all layers),

$\Delta q_{r,k}$ – Displacement vector of FE nodes for reference axis r $(\Delta u, \Delta v, \Delta\varphi)$,

ΔQ_k – Vector of external forces at FE nodes $(\Delta N, \Delta T, \Delta M)$,

$\Delta Q^*_{\mathbf{c,k}}$ – Vector of fictitious forces at FE nodes $(\Delta N^*, \Delta T^*, \Delta M^*)$ arising from concrete flow and shrinkage.

To model the entire construction system, it is essential to establish a FE network. In such a network, the stiffness matrix and force vectors (9) of all FEs are combined in accordance with the principles of FEM (finite element method), connecting nodes within the overall network of FEs. By solving the system of algebraic equations, we can determine the global displacement vector of the nodes, subsequently allowing for the analysis of the required deformation components for each FE within their local systems:

$$\left|\begin{matrix}\Delta\varepsilon_r \\ \Delta\kappa\end{matrix}\right|_k = \mathbf{B}_{r,k} \cdot \mathbf{\Delta q}_{r,k} + \left|\begin{matrix}\Delta\varepsilon_N \\ -\Delta\kappa_M\end{matrix}\right|_k \tag{10}$$

Where:

$\Delta\varepsilon_{N,k}$ – Part of the deformation resulting from the averaging of fictitious normal forces of the observed FE,

$\Delta\kappa_{M,k}$ – Part of the curvature originating from the external distributed load in the element's field, transformed into nodes.

The total stresses and strains for a discrete moment in time are determined through a step-by-step superposition process [38].

Settings for the Coupled Beam Analysis

Based on the longitudinal and transverse cross-section of the bridge (Figure 2), it was assumed for the static calculation that the continuous span beam consists of a steel beam (SB) of varying cross-section and a subsequently cast concrete slab, which forms a composite T-section (Figure 3). Simultaneously, SB is longitudinally extended using a system of segmental cantilever construction in three phases, symmetrically on both sides of the bridge (Figure 4). After that, the slab is reinforced and cast, also symmetrically by segments in three phases (Figure 4), starting with the central segment and then the segments towards the ends of the bridge, every 10 days. The paving and other finishing works complete the construction of the bridge, which introduces an additional permanent (dead) and moving (live) load (Figure 4). All the aforementioned phases of construction define a possible change in the static system and in the geometry of the elements, as well as a change in the load and rheology of concrete.

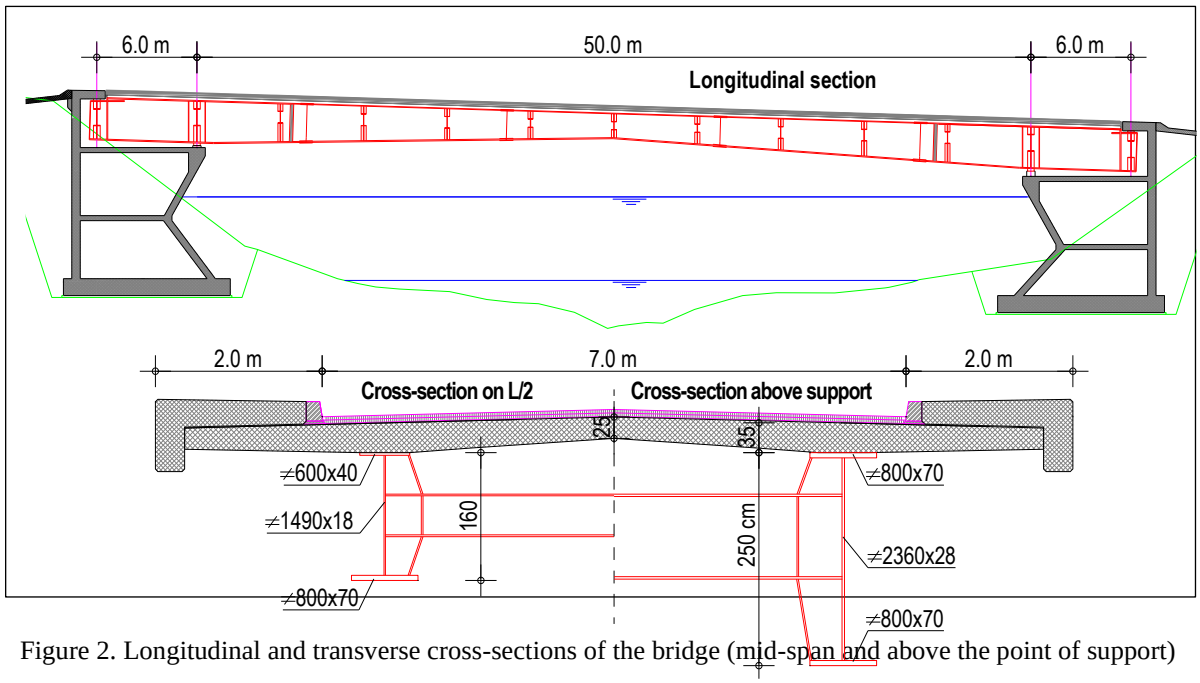

Figure 2. Longitudinal and transverse cross-sections of the bridge (mid-span and above the point of support)

The data necessary for the analysis (material characteristics, phased loads, and element geometry) are given in the figures. Figure 4 illustrates the static systems and loads across different time intervals. The activation of the load and the adjustment of the FE stiffness align with the actual conditions during the phased segmental construction and bridge operation.

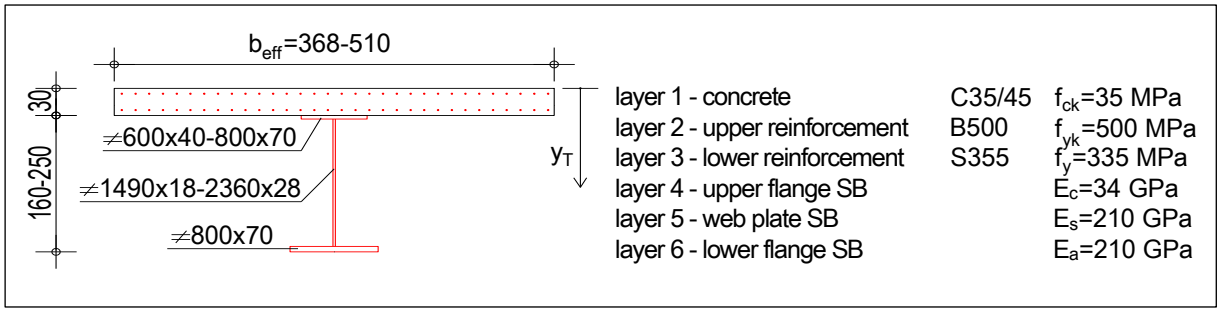

Figure 3. Alternative cross – sections of the composite beam

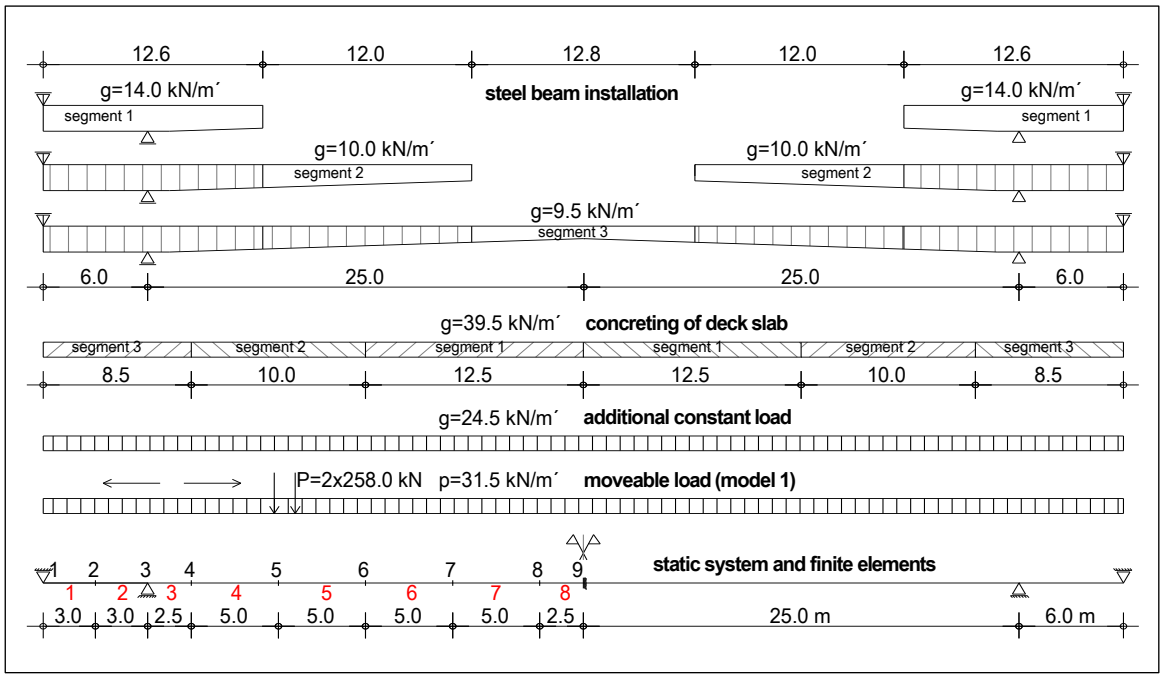

Figure 4. Phases of steel beam installation and slab casting,
additional dead and live loads, static system, and finite elements

The analysis of the span structure of the bridge with the introduced rheological properties (rheology) of concrete was carried out for the period from the beginning of construction up to 10,000 elapsed days, and for different states of stiffness of the concrete slab (non-cracked and cracked zone of tensioned concrete). In doing so, the total time period was divided into 14 intervals in accordance with the adopted construction technology and the load on the span structure of the bridge (Table 1). The finite elements (FE) mesh was formed for half of the symmetrical beam, and the corresponding geometric characteristics of the elements were calculated for them (Figures 3 and 4).

Table 1. Flow of calculation analysis of the characteristic construction phases

Time		Flow of activities	FE/layer
$\Delta t_1=0$	$t_1=0$	Fitting of SB – segment 1	(1-4)/(4-6)
$\Delta t_2=0$	$t_2=0$	Fitting of SB – segment 2	(1-6)/(4-6)
$\Delta t_3=0$	$t_3=0$	Fitting of SB – segment 3	(1-8)/(4-6)
$\Delta t_4=0$	$t_4=10$	Concreting – segment 1	(1-8)/(4-6)
$\Delta t_5=10$	$t_5=20$	Concrete Rheology (time-dependent changes)- segment 1	(1-5)/(4-6) (6-8)/(1-6)
$\Delta t_6=0$	$t_6=20$	Concreting – segment 2	(1-5)/(4-6) (6-8)/(1-6)
$\Delta t_7=10$	$t_7=30$	Concrete Rheology (time-dependent changes)- segment 1+2	(1-3)/(4-6) (4-8)/(1-6)
$\Delta t_8=0$	$t_8=30$	Concreting – segment 3	(1-3)/(4-6) (4-8)/(1-6)
$\Delta t_9=25$	$t_9=25$	Concrete Rheology (time-dependent changes)- segment 1+2+3	(1-8)/(1-6)
$\Delta t_{10}=0$	$t_{10}=25$	Additional dead load	(1-8)/(1-6)
$\Delta t_{11}=310$	$t_{11}=365$	Concrete Rheology (time-dependent changes)	(1-8)/(1-6)
$\Delta t_{12}=635$	$t_{12}=1000$	Concrete Rheology (time-dependent changes)	(1-8)/(1-6)
$\Delta t_{13}=9000$	$t_{13}=10000$	Concrete Rheology (time-dependent changes)	(1-8)/(1-6)
$\Delta t_{14}=0$	$t_{14}=10000$	Live load	(1-8)/(1-6)

The rheological characteristics of the beam concrete were calculated in accordance with EC2. In this case, for RH=80%, the maximum values of the coefficient of creep and shrinkage were assumed to be $\varphi_{(\infty,10)} = 1.75$ and $\varepsilon_{cs(\infty,10)} = 0.24$ ‰ respectively. All intermediate values, for the relative time relations between discrete moments, are calculated as increments. The calculation analysis was carried out using the established computer algorithm.

The concrete slab with creep and shrinkage properties was calculated assuming different ages of concrete and non-cracked and cracked variants.

ANALYSIS OF CALCULATION RESULTS

After the analysis, the results are provided in the form of deflection diagrams along the beam and stress diagrams in relevant cross-sections (mid-span and support cross-section) for cracked and non-cracked concrete in the tensioned support zone (Figures 5-9).

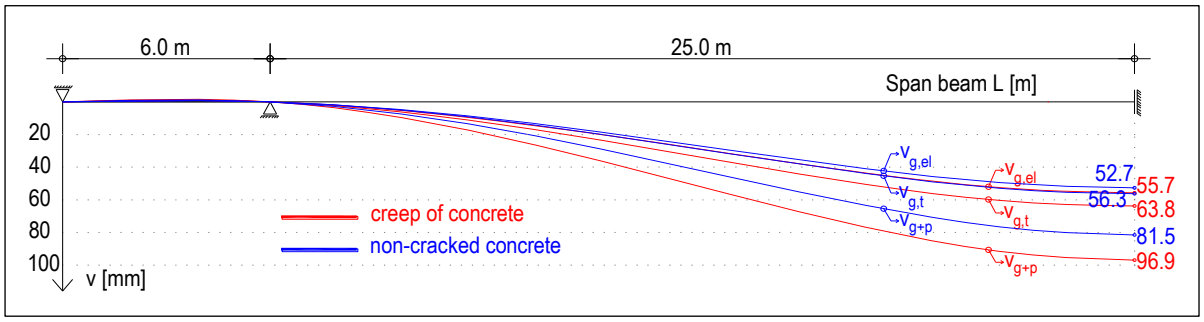

Figure 5. Deflections along the composite beam

Deflections along the beam, with all discrete intervals summed up ($\Delta t_1 + \Delta t_2 + \Delta t_3 + \Delta t_4 + \Delta t_6 + \Delta t_8 + \Delta t_{10}$) which include the elastic discontinuous effects of the dead load, have the expected values. In the middle of the range for sprayed concrete (Figure 5), this deflection is $v_{g,el}$=55.7 mm, which corresponds to approximately L/900. The effects of shrinkage and flow in the pressed concrete contributed to an increase in deflection of 14.5%, resulting in a value of $v_{g,t}$=63.8 mm.

When considering the impact of a moving load, the total deflection at L/2 is v_{g+p}=96.9 mm (approximately L/500). This deflection needs to be elevated with the camber level in the phase of fitting the segments of the plate supports. In the case of the non-cracked concrete, the deflections are lower, so in L/2, this deflection is v_{g+p}=81.5 mm, which is a decline of 16% compared to the state of the cracked concrete (Figure 5).

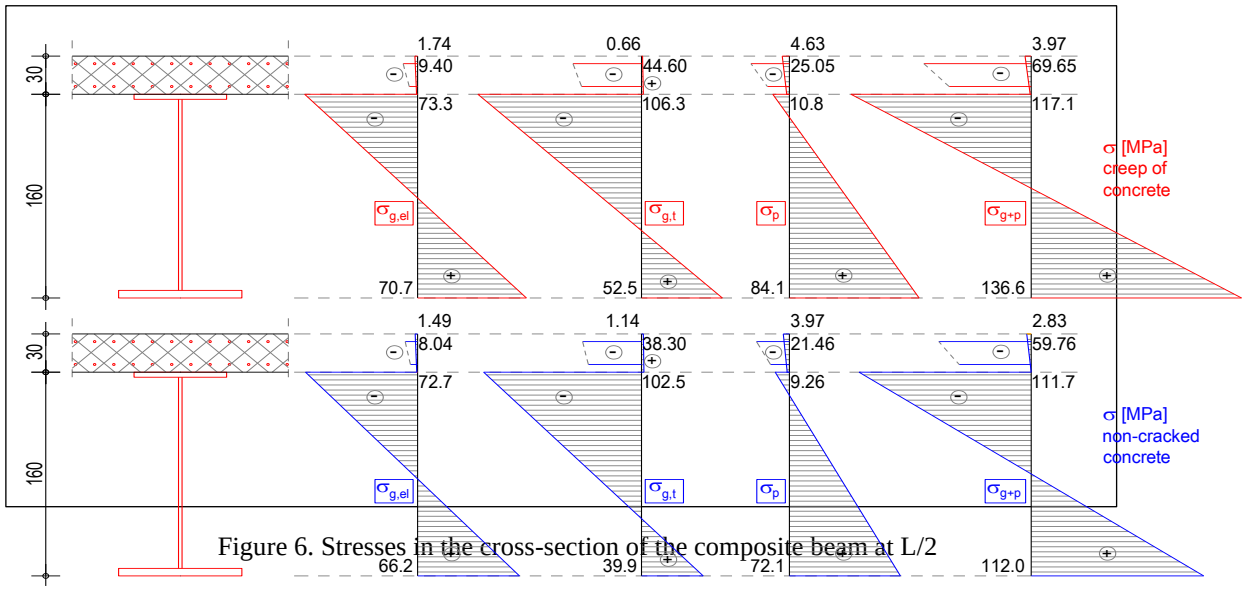

Figure 6. Stresses in the cross-section of the composite beam at L/2

When it comes to the normal stresses in the mid-span cross-section of the cracked tensioned concrete (Figure 6), a significant influence of the viscous behaviour of concrete on the change of these stresses in all layers of the section is visible.

The concrete layer was unloaded to such an extent that it went from a slightly compressed state to a tensile state (from -1.74 to +0.66 MPa), and due to this redistribution of the stress, the reinforcement in the concrete and the top flange LN suffered a significant increase in compressive stress (reinforcement from -9.40 to - 44.60 MPa which is an increase of 4.7 times, the top flange from -73.3 to -106.3 MPa, which is an increase of 45%). At the same time, the tensile stresses on the bottom flange LN decreased (from +70.7 to +52.5 MPa, which is a decrease of 25.7%).

These stresses, summed up with the contribution of the live load, indicate a sufficient reserve in terms of the utilization of individual layers/materials for normal stresses. For non-cracked concrete, the stresses in all layers are lower compared to the condition of the cracked tensioned concrete (Figure 6).

When it comes to the redistribution of stresses in L/2 over time (Figure 7) it is visible that the changes are more intensive in the initial intervals, when the concrete is less aged, in contrast to the slower increase of the aged concrete, for example, after 3 years.

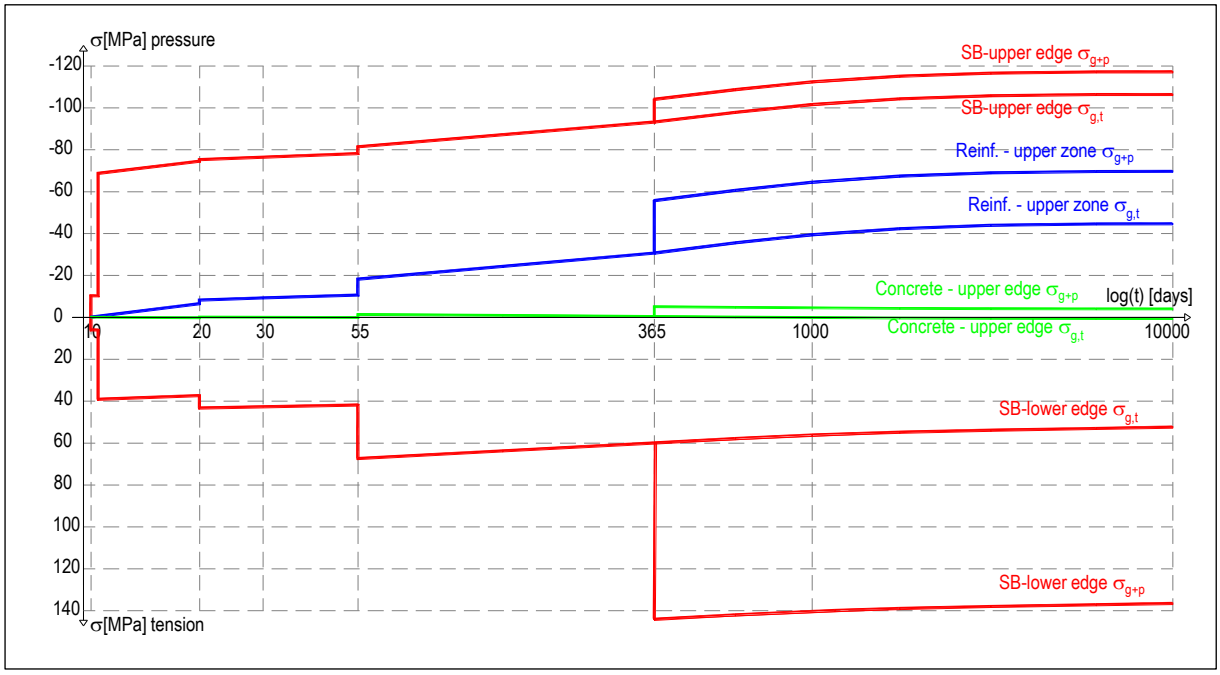

Figure 7. Stresses in the cross-section in L/2 over time, cracked tensioned concrete

In the case of normal stresses of the cross-section of the support (Figure 8), a slightly smaller influence of the viscous behaviour of concrete on the change of these stresses was recorded compared to the cross-section in L/2. This is somewhat expected considering that the tensioned cracked layer, which is excluded from the bearing capacity, is located directly above the observed support cross-section. In all other active layers, the normal stresses increased (reinforcement from +27.9 to +40.3 MPa, which is an increase of 44.4%, top flange from +97.2 to +109.7 MPa, which is an increase of 12.9%, bottom flange from -103.4 to -118.7 MPa, which is an increase of 14.8%).

These stresses, summed up with the contribution of the live load, indicate the efficient utilisation of individual layers/materials for normal stresses. For non-cracked tensioned concrete, the stresses in all layers are lower compared to the state of the cracked concrete (Figure 8). This especially applies to the upper layers closer to the active concrete (reinforcement and top flange LN), which is why the neutral axis is significantly shifted upwards.

When it comes to the redistribution of stresses in the support cross-section over time (Figure 9), as in the L/2 cross-section, the changes are more intensive when the concrete is less aged, in contrast to the slower increase of the aged concrete, e.g., after 2-3 years

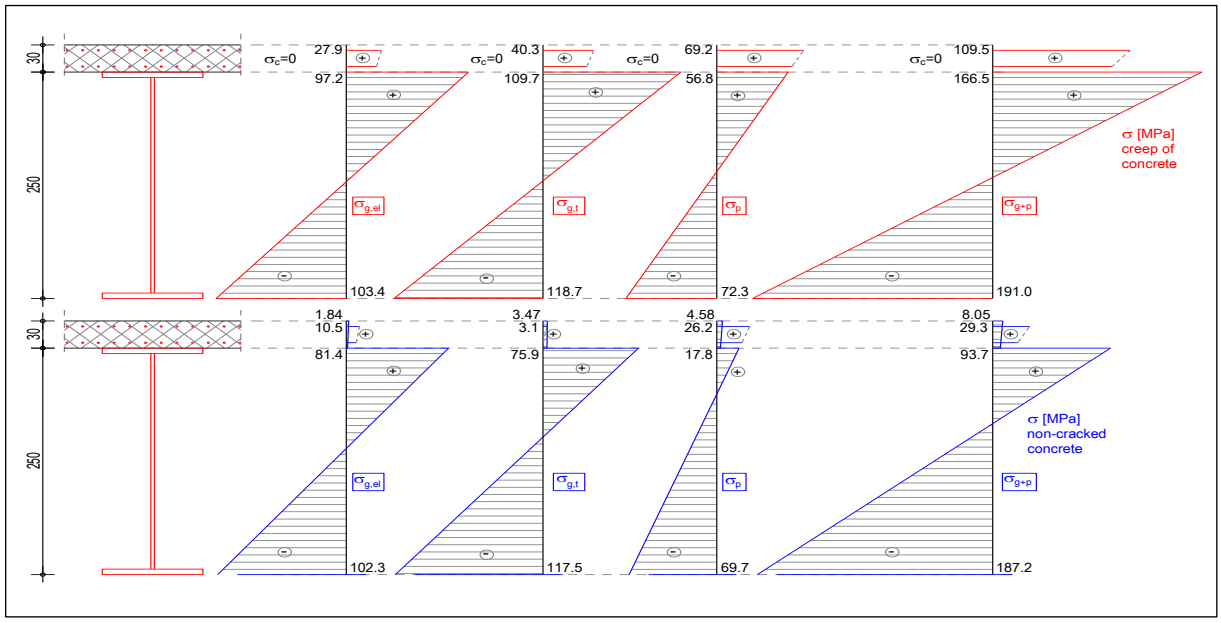

Figure 8. Stresses in the cross-section of the composite beam support

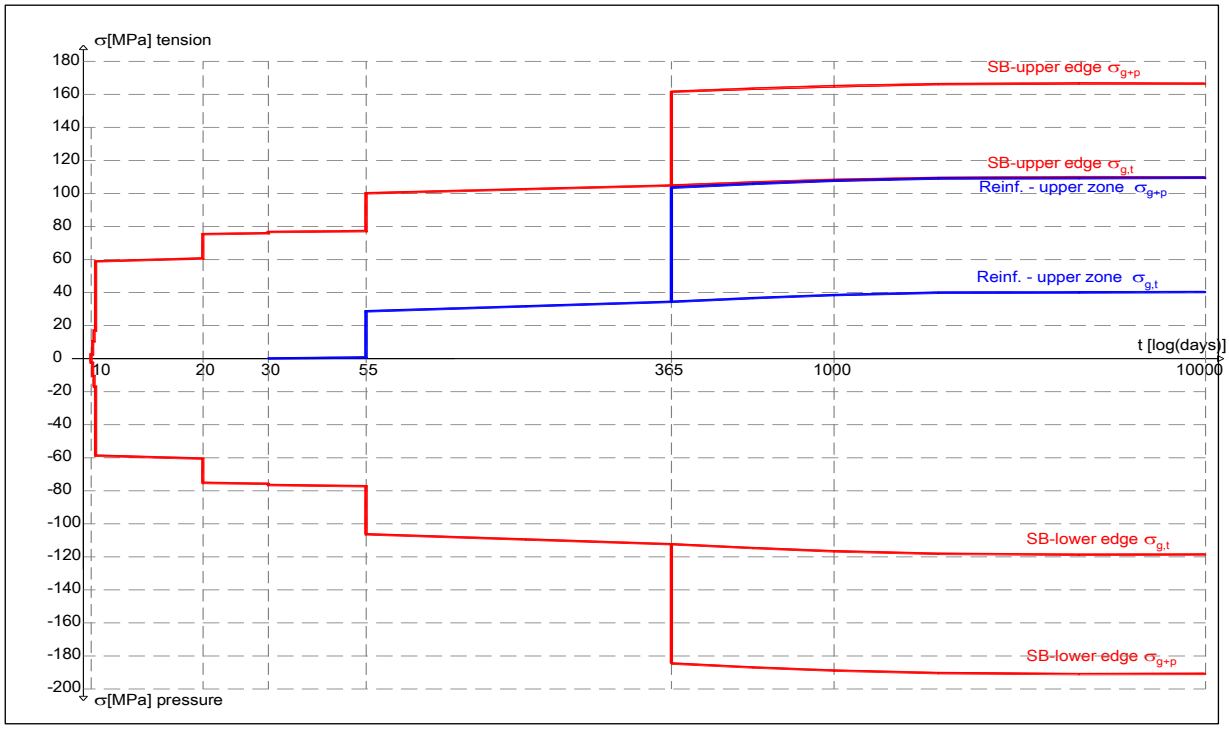

Figure 9. Stresses in the cross-section above the support over time, cracked tensioned concrete

In general, the presented calculation analysis results show that the viscous properties of the concrete slab caused a considerable redistribution of stress between the composite layers along the span of the bridge beam. At the same time, this redistribution takes place in the form of unloading of concrete and additional stress of the steel parts.

CLOSING REMARKS AND CONCLUSION

The additional analysis of the spanning structure of the bridge, which considers the rheological properties, i.e., shrinkage and creep of concrete included the period from the start of the construction to the age of 27.4 years. The stiffness of the concrete slab is analysed for the cross-section without cracks (according to EN 1994-1-1 [39]) and for the cross-section with cracks in the zone of tensioned concrete.

In concrete without cracks, the stresses in all layers are lower compared to the condition with cracks in the tensioned zone. It is shown that the redistribution of the stress, mid-span, is more intensive over time for the less aged concrete. However, even the stresses obtained in this way are within the permissible limits, and at the same time, they were conservative in terms of safety, in the procedure of beam designing.

Based on the analysis results of the coupled bridge in question, it can be concluded that the designed structure meets all safety, economic, and aesthetic requirements. Yet, it was shown that, in order to obtain a more realistic understanding of the behaviour of the composite spanning beam over time, it is necessary to include the creep and shrinkage of concrete in the design. The time-dependent of stresses and deformations considerably contribute to their redistribution, which is necessary to take into consideration when designing the structure. It is also demonstrated that it is not justified to introduce the full stiffness of tensioned concrete in the analysis, because one may obtain results that considerably depart from the actual status.

The design mode according to FEM (developed by the author) employed in the case study, in the framework of the introduced assumptions, makes it possible to analyse different cases in engineering practice when it comes to the control of the limit states of serviceability. The model is generalized and includes statically indeterminate structures with the rigidly composed layer elements. In the process, the real procedures during construction and operation are introduced, in the form of the change of the static system, load, geometry, and rheological properties of the beam.

Received September 2023, accepted October 2023)

REFERENCES

[1] Ranzi, G., Leoni, G., Zandonini, R.: State of the art on the time-dependent behaviour of composite steel-concrete structure, Journal of constructional steel research, 80, 2013, 252-263.
[2] Ding, M., Jiang, X., Lin, Z:, Ju, J.: Long-term stress of simply supported steel-concrete compozite beams, The Open Construction and Building Technology J., 2011, 5, pp. 1-7.
[3] AASHTO LRFD Bridge design specifications, SI Units, 4th Edition, 2007.
[4] Eurocode 2: 2004. Design of Concrete Structures – part 1-1: General rules and rules for buildings – EN 1992-1-1:2004, European Committee for Standardization, Brussels.
[5] Eurocodes 3 and 4 – Application to steel-concrete composite road bridges, Guidance book, Sétra, Department of the French Ministry of transport, France, 2007.
[6] El Sarraf, R., Iles, D., Montahan, A., Easey, D., Hicks, S.: Steel-concrete composite bridge design guide, NZ Transport Agency research report 525, September 2013.
[7] CEB-FIP: Model Code 1990, T. Telford, London, 1993.
[8] FIB Model Code 2010, Paris, 2013.
[9] ACI 209R-02: Prediction of creep, shrinkage, and temperature effects in concrete structures. ACI Committee, 2002.
[10] Mathematical Modeling of Creep and Shrinkage of Concrete, Ed. Z. Bažant, A. A Wiley- Int.. Public. 1988.
[11] Partov, D., Kantchev,V.: Eurocode 2 provision against standards (ACI 209R-92 and Gardner&Lockman models) in creep analysis of composite steel-concrete section, Engineering Mechanics, Vol. 22, 2015, No. 2, pp. 109-127.
[12] Vayas, I., Iliopoulos, A.: Design of steel-concrete comosite bridges to eurocodes, CRC Press, 2014.
[13] Hendy,C.R., Johnson, R:P.: Designers guide to EN 1994-2 Eurocodes 4: Design of steel and comosite structures, Part 2: General rules and rules for bridges, 2004.
[14] Al-Darzi, S.Y., Chen, A.: Conceptual design and analysis of steel-concrete comosite bridges: State of the Art, Steel Strustures, 2006, pp. 393-407. www.kssc.or.kr

[15] Folić R., Radonjanin, V., Malešev, M.: „Design and Analysis of Steel-Concrete Composite Structure“, Introductinary - Invited paper on 6th Greek National Conference on Metal Structures, Athens: Greek Association for Metal Structures, 2008, pp. 72 – 87.
[16] Sassone, M., Casalegno, C.: Evaluation of the structural response to the time-dependent behaviour of concrete: Part 2 – A general computational approach, ICJ The Indian Concrete Journal, 86, 2012. 12, 39-51.
[17] Wang, G-M., Zhu, L., Zou, G-P., Han, B., Ji, W-Y.: Experimental research of the time-dependent effects of steel-concrete composite girder bridges during construction and operation periods, MDPI Materials, 2020, 13, 2123, doi:10.3390/ma13092123
[18] Cardoso, R. A: Design of comosite steel and concrete bridges, Univeridade de Aveiro Dep. de Eng. Civil, Arno 2015.
[19] Kim, S.: Creep and shrinkage effects on steel-concrete composite beams, Master Thesis.
[20] Kostić, S., Deretić-Stojanović, B., Stošić, S.: „Redistribution effects in linear elastic analyses of continuous composite steel-concrete beams according to Eurocode 4“, Facta Universitatis, Series: Architecture and Civil Engineering,Vol. 9, No 1, 2011, pp. 133-145.
[21] Nguyen, Q-H. Hjiaj, M.: Nonlinear time-dependent behaviour of composite steel-concrete beams, Hal, April 13, 2015.
[22] Chiorino, M.A., Carreira, D.J.: Factors affecting creep and shrinkage os hardened concrete and guide for modelling, ICJ The Indian Concrete Journal, vol.86, No.12, Theme: Creep and Shrinkage, A state-of-the-art report on international recommendations and scientific debate, Maharashtra, India, 2012, pp. 11-24.
[23] Collin, P., Nilsson, M., Häggström, J.: International Workshop on Eurocode 4-2, Composite Bridges, Technical report, Stockholm, 2011.
[24] Macorini, L., Fragiacomo, M., Amadio, C., Izzuddin, B.A.: Long-term analysis of steel-concrete composite beams; FE modelling for effective with evaluation, Engineering Structures,, 28, 2006, pp. 1110-1131.
[25] Gara, F., Leoni, G. Dezi, L.: A beam finite elerment including shear lag effect for the time-dependent analysis of steel-concrete composite decks, Eng. Struct., 31, 2009, pp. 1888-1902.
[26] Reginato, L.H., Tamoyo, J. L., Morsch, I. B.: Finite element study of effective width in steel-concrete composite beams under long-term service load, Latin Amer. J. of Solid and Structures, 2018,15(8), 15 p.
[27] Bradford, M.A., Gilbert,R.I.: Time-dependent behaviour of simply supported steel-composite beams, The University of New South Wales, SCE, UNICIV Report No. R-286 July 1991.
[28] Dezi, L., Leoni, G., Tarantino, A.M.: Creep and shrinkage analysis of composite beams, Composite construction, Constr. Research Communications Limited, 1998, pp. 170-177.
[29] Souici, A., Tehrani, M., Rahal, N., Bekkouche,M.S. Berehet: Creep effect on composite beam with perfect steel-concrete connection, Steel structures, 15, 2, 2015, pp. 433-445.
[30] Fragiacomo,M., Amadio, C., Macorini, L.: Finite-element model for collapse and long-term analysis of steel-concrete composite beams, ASCE, Journal of structural engineering, March, 2004, pp. 489-497.
[31] Chen, F., Ai, Z., Wang, C., Hou, S.: Research on simulation method of steel-concrete composite beam with finite element, IOP Conf. Series: Earth and Enviromental Science, 719, 2012, 022035; doi:10.1088/1755-1315/719/2/022035
[32] Gholamhoseini, A., Gilbert, R.I., Bradford, M.A.: A simplified method for calculation of long-term deflections in composite slabs, Steel Innovationa, 2015, Auckland, N. Zealand, 3-4 September 2015.
[33] Yao, K., Zhou, D. He, Y., Wu, S.: The simplified algorithm to the simple-supported steel and concrete comosite beam, Hindawi, Computational Inteligence and Neuroscience, Vol. 2022, Article ID 4951080, 10 p.
[34] Zhang, C., Shao, C. Su, Q. Changyuan, D.: An experimental study on negative banding behaviour of composite bridge decks with steel-fiber-reinforced concrete and longitunal buld-flat ribs, I. J. of steel structures, 16 March 2023.
[35] Niu, Y., Tang, Y.: Effect of shear creep on long-term deforoamtion analysis of long span concrete girder bridge, Hindawi, Advances in Materils Science aand Engineering, Vol. 2019, Article ID 4382904, 10 p. https://doi.org/10.1155/2019/4382904
[36] Morano, S. G., Mannini, C.: PreflexBeams: A method of calculation of creep and shrinkage effects, ASCE, Journal of Bridge Engineering, January/february 2006, pp. 48-58.
[37] Cumbo, A., Folić, R.: Layered finite elements in the analysis of composite structures exposed to long-term effect, Građevinar, 69, 2017, No. 11, Zagreb, 2017, pp. 991-1005.
[38] Cumbo, A.: Analisis rheollogical properties influences of composite structures by layered finite elements, Ph Thesis, Faculty of Civil Engineering and Architecture, Niš, 2017. (in Serbian).
[39] Johnson, R:P. Composite structures of steel and concrete, Blackwall P., Therd Edition, Oxford, 2004.